Science of the Total Environment 675 (2019) 581–593

Contents lists available at ScienceDirect

Science of the Total Environment

journal homepage: www.elsevier.com/locate/scitotenv

Relevance of carbon burial and storage in two contrasting blue carbon ecosystems of a north-east Pacific coastal lagoon

Tomasa Cuellar-Martinez [a], Ana Carolina Ruiz-Fernández [a,*], Joan-Albert Sanchez-Cabeza [b], Libia-Hascibe Pérez-Bernal [a], Jose Sandoval-Gil [c]

[a] Unidad Académica Mazatlán, Instituto de Ciencias del Mar y Limnología, Universidad Nacional Autónoma de México, 82040 Mazatlán, Sinaloa, Mexico
[b] Unidad Académica Procesos Oceánicos y Costeros, Instituto de Ciencias del Mar y Limnología, Universidad Nacional Autónoma de México, Ciudad Universitaria, 04510 Ciudad de México, Mexico
[c] Instituto de Investigaciones Oceanológicas, Universidad Autónoma de Baja California, Carretera Transpeninsular Ensenada-Tijuana No. 3917, Frac. Playitas, 22860 Ensenada, Baja California, Mexico

HIGHLIGHTS

- C_{org} accumulation was analyzed in ^{210}Pb-dated seagrass and salt marsh sediment cores.
- C_{org} accumulated faster but at lower amount in seagrass than in salt marsh habitats.
- Land use changes promoted variation in sediment accumulation and C_{org} burial rates.
- C_{org} stocks from both habitats offset the annual CO_2 emission of a medium-sized city.

GRAPHICAL ABSTRACT

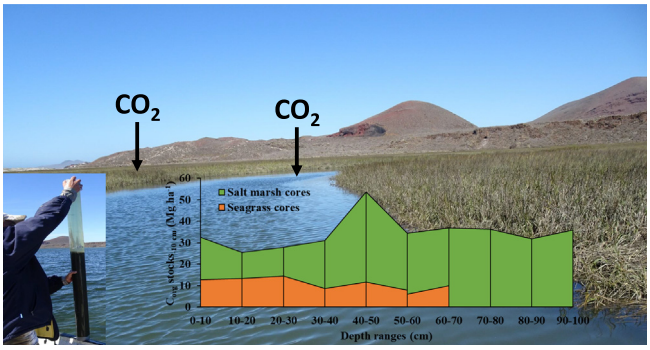

ARTICLE INFO

Article history:
Received 24 January 2019
Received in revised form 24 March 2019
Accepted 24 March 2019
Available online 29 March 2019

Editor: Damia Barcelo

Keywords:
Blue carbon ecosystems
California Current Large Marine Ecosystem
Spartina foliosa salt marsh
Zostera marina seagrass
^{210}Pb chronology
Coastal sediments

ABSTRACT

Coastal vegetated ecosystems constitute very productive habitats, characterized by efficient C_{org} sequestration and long-term preservation in sediments, so they play an important role in climate change mitigation. The temporal evolution of C_{org} content, stocks and burial rates were evaluated in seagrass and salt marsh habitats in San Quintin Bay (northeast Pacific, Mexico) by using ^{210}Pb-dated sediment cores. Salt marsh cores were characterized by fine-grained sediments, higher salinities, lower terrigenous input and lower mass accumulation rates (MAR: 0.01–0.03 g cm^{-2} yr^{-1}) than seagrass cores (MAR: 0.02–3.21 g cm^{-2} yr^{-1}). Accumulation rates in both habitats steadily increased throughout the past century most likely because of soil erosion promoted by land use changes in the surroundings. The C_{org} stocks were highest in salt marsh cores (12.2–53.6 Mg ha^{-1} at 10 cm depth; 259–320 Mg ha^{-1} at 1 m depth) than in seagrass cores (5.7–14.4 Mg ha^{-1}, and 80–98, Mg ha^{-1}, respectively), whereas C_{org} burial rates were considerably lower in salt marsh (13–60 g m^{-2} yr^{-1}) than in seagrass (9–144 g m^{-2} yr^{-1}) habitats, and the temporal variations observed in C_{org} burial rates were mostly driven by changes in the accumulation rates. The overall C_{org} stock (485 ± 51 Gg C) for both habitats together was comparable to the carbon emissions of a major city nearby. Our results highlight the need to protect these environments as relevant carbon reservoirs.

© 2019 Elsevier B.V. All rights reserved.

* Corresponding author.
E-mail address: caro@ola.icmyl.unam.mx (A.C. Ruiz-Fernández).

https://doi.org/10.1016/j.scitotenv.2019.03.388
0048-9697/© 2019 Elsevier B.V. All rights reserved.

1. Introduction

Seagrass meadows, salt marshes and mangrove forests are highly productive vegetated coastal ecosystems that provide significant environmental services, such as sediment stabilization, coastal protection and provision of food and habitat for commercially important marine species (Spalding et al., 2003; Weis et al., 2016 and references therein). These environments, known as "blue carbon" ecosystems (Duarte et al., 2005; Mcleod et al., 2011; Huxham et al., 2018) are efficient carbon sinks and play an important role in climate change mitigation by carbon sequestration (Chmura et al., 2003; Duarte et al., 2005; Fourqurean et al., 2012). Commonly, the largest organic carbon (C_{org}) fraction of plant biomass are roots and rhizomes that, together with the canopy, protect sediments from erosion (Alongi, 2018). The efficient C_{org} storage and long-term preservation in these ecosystems are caused by the slow C_{org} decomposition owing to high sediment accumulation rates that prevent oxygen penetration in the sediments (Duarte et al., 2013; Alongi, 2018) and by the presence of refractory carbon compounds, that differs among tissue types and species (Trevathan-Tackett et al., 2015, 2017a).

Worldwide, coastal ecosystems face multiple threats mainly related to human activities such as urbanization, aquaculture, conversion to farmland, fishing, shipping and coastal engineering. Also, recent climate change, including seawater warming and sea-level rise, threaten these ecosystems and the services they provide (Duarte, 2002; Gedan et al., 2009). Over the past 50 years, 25%–50% of the area covered by vegetated coastal ecosystems has been lost (Duarte et al., 2013), and in some places the loss has been >70% (e.g. Singapore, Bohau Bay, China and southeastern coastal states from United States; Li et al., 2018 and references therein).

The loss and degradation of blue carbon ecosystems cause the decomposition of buried C_{org} and CO_2 emissions to the atmosphere contribute to global warming (Pendleton et al., 2012). Therefore, the protection of coastal vegetated habitats are effective mitigation strategies of climate change, through the reduction of greenhouse gas emissions (Duarte et al., 2013). Globally, the highest C_{org} stocks correspond to mangroves followed by salt marshes and seagrass meadows (Howard et al., 2014; Alongi, 2018). The ongoing sink capacity of these ecosystems can be estimated through the quantification of C_{org} stocks and burial rates. In Mexico, the mangrove area extension is well known (764,486 ha; CONABIO, 2013); however, salt marsh and seagrass meadows have not yet been fully mapped (CEC, 2016; Arellano-Méndez et al., 2016; Mcowen et al., 2017) and data on C_{org} burial rates and stocks in seagrass (Arellano-Méndez et al., 2015; Thorhaug et al., 2019) and salt marshes (e.g. Ruiz-Fernández et al., 2016; Carnero-Bravo et al., 2016, 2018; Bojórquez-Sánchez et al., 2017; Burke Watson and Hinojosa Corona, 2018; Ruiz-Fernández et al., 2018) are still very scarce.

The purpose of this work was to evaluate the temporal evolution of C_{org} concentrations (%), stocks (Mg ha^{-1}) and burial rates (g cm^{-2} $year^{-1}$) in seagrass and salt marsh sediment cores from San Quintin Bay (Mexican North Pacific coast), under the hypotheses that main economic activities developed in the surroundings of the study area (agriculture and aquaculture) might have affected C_{org} burial and stocks within the past.

2. Material and methods

2.1. Study area

San Quintín Bay (SQB, 30°27′ N; 116°00 W) is a shallow lagoon (extension ~48 km^2 – Ward et al., 2004) with average depth ~2 m, in the northern Pacific coast of the Baja California peninsula (Fig. 1). It consists of two sub-basins: west and east arms, with extensive intertidal and subtidal shoals and channels up to about 10 m deep extending the length of each arm (Aguirre-Muñoz et al., 2001). It was designated as Ramsar site on 2008, it is the habitat for numerous endemic animal and plant species, and it is an important reproduction and wintering site for diverse bird species (Martínez-Ríos, 2007). The climate is very dry, with rainfall restricted from November to March. The mean annual rainfall from 1957 to 2008 was 162 mm, and the air temperature ranged from 9.7 to 22.8 °C (Santa María del Mar meteorological station; SMN, 2018), so it is a net evaporative system with no significant runoff or groundwater inflow (Ibarra-Obando et al., 2001). SQB surface sediments have a high content of plagioclase and quartz, with low K-feldspar. The main mineral sources are from the local San Quintín Volcanic Field and from the erosion of the batholitic basement (Daesslé et al., 2009).

SQB, in the California Current Large Marine Ecosystem, is influenced by coastal upwelling. This mainly occurs in late spring and summer (Álvarez-Borrego, 2004), when strong northerly and northwesterly alongshore winds induce offshore transport of surface water, resulting in upwelling of cool and nutrient-enriched deep waters (Ibarra-Obando et al., 2001), which are propagated in SQB by tidal currents (Zaytsev et al., 2003).

The main marine habitats in SQB are seagrass, salt marsh, intertidal mudflat and deep mud in the channels (Ward et al., 2003; Ibarra-Obando et al., 2004). The dominant submerged vegetation is the eelgrass *Zostera marina* L. (19.5 km^2; Ward et al., 2004), also are present some macroalgae species such as *Ulva* sp. *Gracilaria* sp., and *Chondracanthus* sp., (Zertuche-González et al., 2009; Ávila-López et al., 2017) and the widgeongrass *Ruppia* sp. (Ward et al., 2004). The dominant species in salt marshes are *Spartina foliosa* Trin., *Batis maritima* L., *Salicornia* spp. and *Suaeda* spp. (Ward et al., 2004).

The main human activity adjacent to SQB (San Quintín Valley) is agriculture (Aguirre-Muñoz et al., 2001) although agrochemical contamination is not significant (Daesslé et al., 2009). The primary economic activity within the lagoon since 1979 is oyster aquaculture (*Crassostrea gigas* Thunberg; García-Esquivel et al., 2004), which covers ~300 ha and is restricted to the western arm (Aguirre-Muñoz et al., 2001). Zertuche-González et al. (2009) suggested that the oyster cultivation increased nutrient supply and consequent *Ulva* spp. blooms within the lagoon, although there are not consistent evidences (Jorgensen et al., 2010).

2.2. Sampling and sample preparation

Four sediment cores were manually collected in March 2018, by pushing down PVC tubes (1.2 m long and 8.6 cm internal diameter) at two seagrass (P1: 70 cm; P2: 60 cm) and two salt marsh (M1: 98 cm; M2: 100 cm) areas in the western arm of SQB (Fig. 1). The sampling sites were selected based on accessibility and closeness to the lagoon mouth and to the aquaculture areas in the surroundings, avoiding dredged or stream influenced areas and navigation channels to minimize the risk of collecting disturbed sediments. The core length varied as the result of sediment characteristics (sandy sediments in seagrass areas offered more resistance to coring tube penetration than silty sediments in the salt marsh areas). The dominant species in the collection sites were *S. foliosa* Trin., *Salicornia* spp. and *B. maritima* L. in salt marshes, and *Z. marina* L. in seagrass meadows. Sediments were extruded within one day after sampling, and sliced at 1 cm intervals for the upper 50 cm, and at 5 cm intervals below. The sediment samples were weighed before and after freeze-drying, ground into powder with agate mortars (except the aliquots for grain size analyses) and kept in plastic bags at laboratory room temperature (20 °C).

2.3. Laboratory analysis

Total ^{210}Pb ($^{210}Pb_{tot}$) activities were determined through its radioactive descendant ^{210}Po by alpha spectrometry (Ortec Ensemble; Ruiz-Fernández and Hillaire-Marcel, 2009). High-resolution low-background gamma spectrometry (Ortec HPGe well detector) was used to determine ^{137}Cs activities to validate the ^{210}Pb-derived age models. Supported ^{210}Pb ($^{210}Pb_{sup}$) was determined from constant $^{210}Pb_{tot}$ values in each core bottom. Age models, mass accumulation rate (MAR, g cm^{-2} yr^{-1}) and sediment accumulation rate (SAR, cm

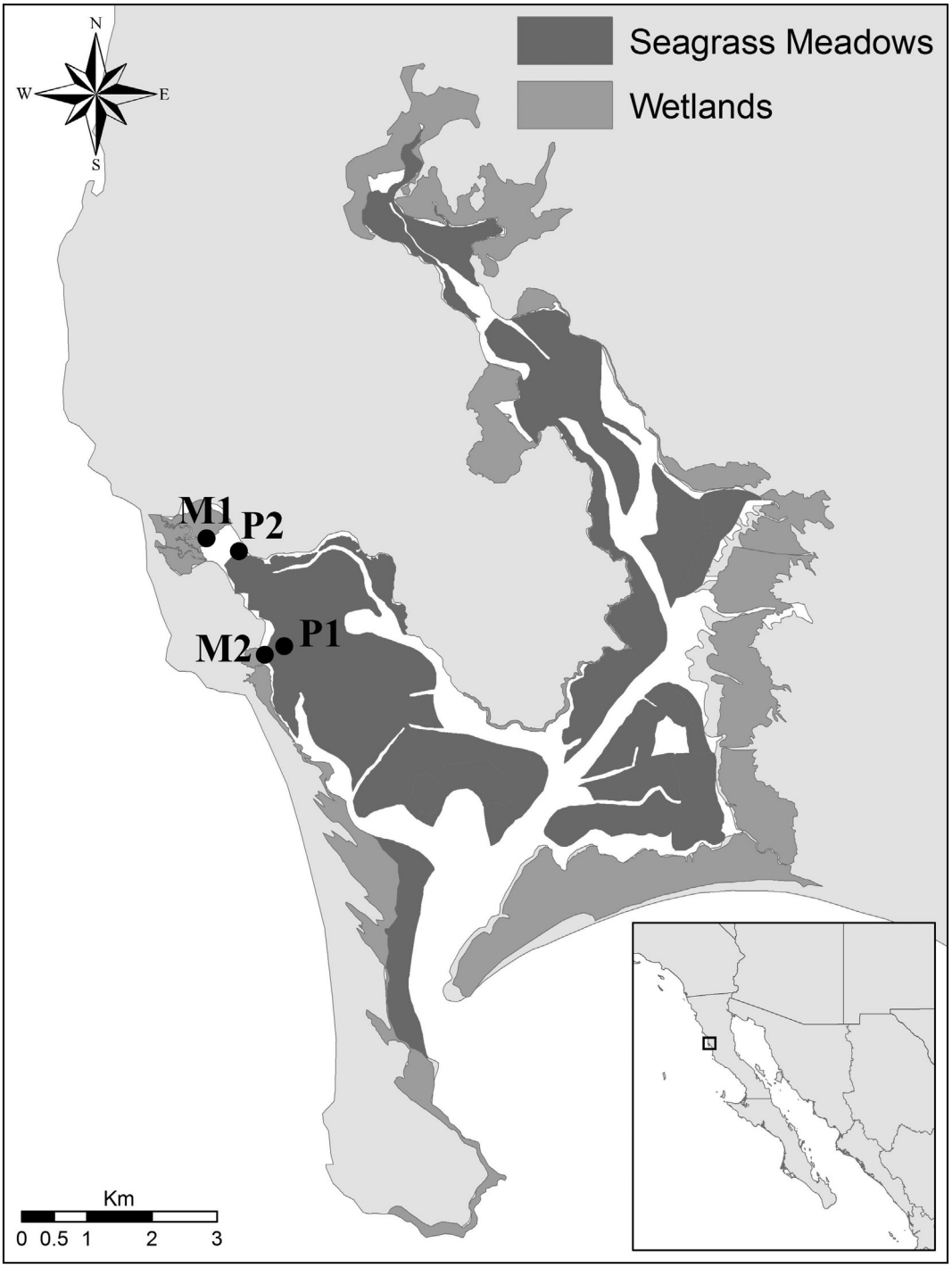

Fig. 1. Study area and collection sites of sediment cores. Salt marsh cores: M1 and M2. Seagrass cores: P1 and P2.

yr^{-1}) were obtained by using excess ^{210}Pb activities ($^{210}Pb_{ex} = {}^{210}Pb_{tot} - {}^{210}Pb_{sup}$) and the Constant Flux (CF) model (Sanchez-Cabeza and Ruiz-Fernández, 2012); following Sanchez-Cabeza et al. (2014), the uncertainties were computed by Monte Carlo simulation with 30,000 iterations (Sanchez-Cabeza et al., 2014).

Sediment grain size distribution was determined by laser diffraction of samples treated with H_2O_2 (30%) to remove organic matter. Elemental composition was determined by X-ray fluorescence (XRF; Spectro Xepos). Magnetic susceptibility (MS) was measured using a Bartington MS2 system coupled to a simple frequency sensor MSG2. Total and organic C and N concentrations were determined with an elemental analyzer (Elementar-Vario Micro Cube). The organic fractions (C_{org} and N_{org}) were determined in carbonate-free samples, treated by successive additions of 1 M HCl, and the inorganic carbon concentrations (C_{inorg}) were estimated by the difference between C_{tot} and C_{org} concentrations.

Analysis of reference materials provided results within the reported range of the certified values: IAEA-300 (Radionuclides in Baltic Sea sediment, International Atomic Energy Agency) for ^{210}Pb and ^{137}Cs activities, IAEA-158 (Trace elements and methylmercury in marine sediment, International Atomic Energy Agency), PACS-2 (Marine sediment reference materials for trace metals and other constituents, National Research Council Canada), LKSD-1 (Lake sediment samples, Natural Resources Canada) and IAEA-433 (Trace elements and methylmercury in marine sediment, International Atomic Energy Agency) for

elemental concentrations, QAS3002 (Quality audit standard, Malvern™) for grain size percentages, and Leco 502 309 (Soil sample, Leco Corporation) for carbon and nitrogen analysis. Replicate analysis of a single sample ($n = 6$) yielded coefficients of variation <10% for ^{210}Pb activities, <3% for elemental composition, <10% for grain size distribution, and <4% for C_{org} and N_{org}.

The amount of C_{org} per unit area at a defined sediment depth (section C_{org} stock) was calculated as the product of dry bulk density, C_{org} concentration and section thickness (Howard et al., 2014) and reported as the sum at every 10 cm (C_{org} stock-$_{10cm}$). Based on the almost constant C_{org} concentrations in the lower segments of the cores, suggesting negligible C_{org} degradation with time (Ruiz-Fernández et al., 2018), we extrapolated the C_{org} stock to 1 m depth (C_{org} stock$_{-1m}$) by using the average C_{org} stock of segments 49–70 cm in P1, 49–60 cm in P2 and 80–85 cm in M1 (no extrapolation was needed in core M2). The carbon burial rates were calculated by multiplying C_{org} concentrations by ^{210}Pb-derived MAR. The C_{org} stock and burial rates uncertainties were estimated by quadratic uncertainty propagation.

2.4. Data analysis

Shapiro-Wilk test confirmed that data set was not normally distributed; thus, non-parametric tests were used. Spearman correlation was performed to determine the associations among variables analyzed. The differences in geochemical composition and C_{org} stocks among cores were assessed through Kruskal-Wallis one-way ANOVA test; and depth variations in C_{org} stock (every 10 cm) among cores was evaluated through a Friedman two-way ANOVA test. In both ANOVA tests, Dunn's multiple comparison was used as a post hoc test. Significance level of $\alpha = 0.05$ was set for all statistical analyses.

To infer sediment provenance and the influence of sediment composition on C_{org} concentrations, a Factor analysis (FA) was performed considering16 variables: grain size (sand, clay, and silt), elemental composition (Al, Ti, Na, Cl, Br, Ca, Zr, Mn and Sr), C_{org}, N_{org} and C_{inorg} concentrations, and magnetic susceptibility (MS); and by using the options of principal component analysis (PCA) for factor extraction and Varimax rotation (significant loadings ≥0.7).

3. Results

3.1. ^{210}Pb activity profiles and ^{210}Pb-derived mass accumulations rates

A summary of ^{210}Pb dating and C_{org} results in sediment cores from SQB is shown in Table 1. ^{210}Pb activities in salt marsh cores were considerably higher (8.9–78.1 Bq kg^{-1}) than in seagrass cores (14.8–36.7 Bq kg^{-1}) (Fig. 2). ^{210}Pb depth profiles in salt marsh cores showed the expected exponential decrease due to radioactive decay, but subsurface maxima were observed at 17.5 cm in core M1 and at 11.5 in core M2 (Fig. 2), not reproduced in the geochemical variable profiles (Section 4.2). These maxima could be the result of accumulation of sediment, with higher concentration of ^{210}Pb, eroded from elsewhere.

In the seagrass cores P1 and P2, ^{210}Pb activities decreased with depth, but displayed irregular profiles (Fig. 2) likely caused by a high variability in sediment supply and/or reflected the high energy common in shallow coastal lagoons. Core P1 showed lower ^{210}Pb activities than core P2, likely resulting from larger sediment supply and higher sand contents in core P1 (Fig. 2).

$^{210}Pb_{sup}$ was estimated from the average activity of ^{210}Pb in the bottom segments. $^{210}Pb_{ex}$ fluxes were consistent for each habitat type. The maximum ^{210}Pb-derived ages were 1905 ± 6 years for core M1, 1915 ± 6 years for core M2, 1929 ± 21 years for core P1 and 1915 ± 9 for core P2. Maximum ^{137}Cs activities were observed as follows: M1 in section 8–9 (1953–1964); M2 in section 7–8 cm (1950–1965); P2 in section 21–22 cm (1964–1967), thus validating the ^{210}Pb age models. Although no clear ^{137}Cs maximum was observed in core P1, the profile showed activities higher than the detection limit only above 47 cm (1954 ± 12), consistent with the onset of the ^{137}Cs atmospheric fallout.

The accumulation rates in salt marsh cores, MAR (0.01–0.03 g cm^{-2} yr^{-1}) and SAR (0.03–0.22 cm yr^{-1}) were lower than in seagrass cores (MAR: 0.02–3.21 g cm^{-2} yr^{-1}; SAR: 0.02–2.41 cm yr^{-1}). The two salt marsh cores and seagrass core P2 evidenced a steady increase in SAR and MAR throughout the past century, although in M2, the accumulation rates stabilized and even decreased since the early 1980s (Fig. 3). MAR and SAR peak values were observed in core P1 within the periods 1951–1961 and 1975–1982 (Fig. 3), although uncertainties were high owing to low $^{210}Pb_{ex}$ activities.

Table 1
Summary of ^{210}Pb dating and C_{org} results in sediment cores from San Quintín Bay, Mexico.

	Core M1		Core M2		Core P1		Core P2	
	Range	Mean[a]	Range	Mean[a]	Range	Mean[a]	Range	Mean[a]
Environment	Salt marsh		Salt marsh		Seagrass		Seagrass	
^{210}Pb (Bq kg^{-1})	8.9–78.1	–	6.1–73.3	–	14.8–22.5	–	15.0–36.7	–
$^{210}Pb_{sup}$ (Bq kg^{-1})	–	10.0 ± 0.7	–	14.4±0.2	–	14.9 ± 0.9	–	17.8±1.5
^{137}Cs (Bq kg^{-1})	< 0.6–7.5	–	< 0.3–18.5	–	< 0.5–1.8	–	< 0.4–4.2	–
^{210}Pb flux (Bq m^{-2} yr^{-1})	–	23.9 ± 0.7	–	18.6±0.6	–	103 ± 7	–	102±4
MAR (g cm^{-2} yr^{-1})	0.01–0.03	0.02 ± 0.01	0.01–0.03	0.02±0.01	0.45–3.21	1.02 ± 0.48	0.02–1.19	0.46±0.31
SAR (cm yr^{-1})	0.04–0.17	0.10 ± 0.03	0.03–0.22	0.13±0.05	0.35–2.41	0.88 ± 0.47	0.02–1.11	0.45±0.29
Surface SAR (cm yr^{-1})	–	0.13 ± 0.01	–	0.13±0.01	–	2.4 ± 0.5	–	0.9±0.3
C_{org} (%)	1.36–15.78	8.09 ± 4.02	1.02–19.47	9.86±3.39	0.37–1.20	0.59 ± 0.21	0.45–2.43	1.15±0.59
C:N	10–14	–	10–21	–	4–15	–	7–14	–
$C_{org-10cm}$ (Mg ha^{-1})	12.2–45.9	25.9 ± 0.5	25.4–53.6	34.4±0.7	5.7–11.4	8.2 ± 0.1	7.9–14.4	11.4±0.4
C_{org} burial rate (g m^{-2} yr^{-1})	15.3–45.3	29.7 ± 3.0	13.1–60.2	42.2±4.7	20.5–154.3	58.5 ± 31.7	9.2–144.2	57.9±12.9
C_{org-1m} (Mg ha^{-1})	–	258.7 ± 3.2	–	319.5±2.6	–	80.1 ± 2.5	–	101.7±3.5
Surface C_{org} burial rate (g m^{-2} yr^{-1})	–	28.3±2.2	–	46.6±3.9	–	103.0±23.7	–	134.7±37.9

[a] Mean value and uncertainty.

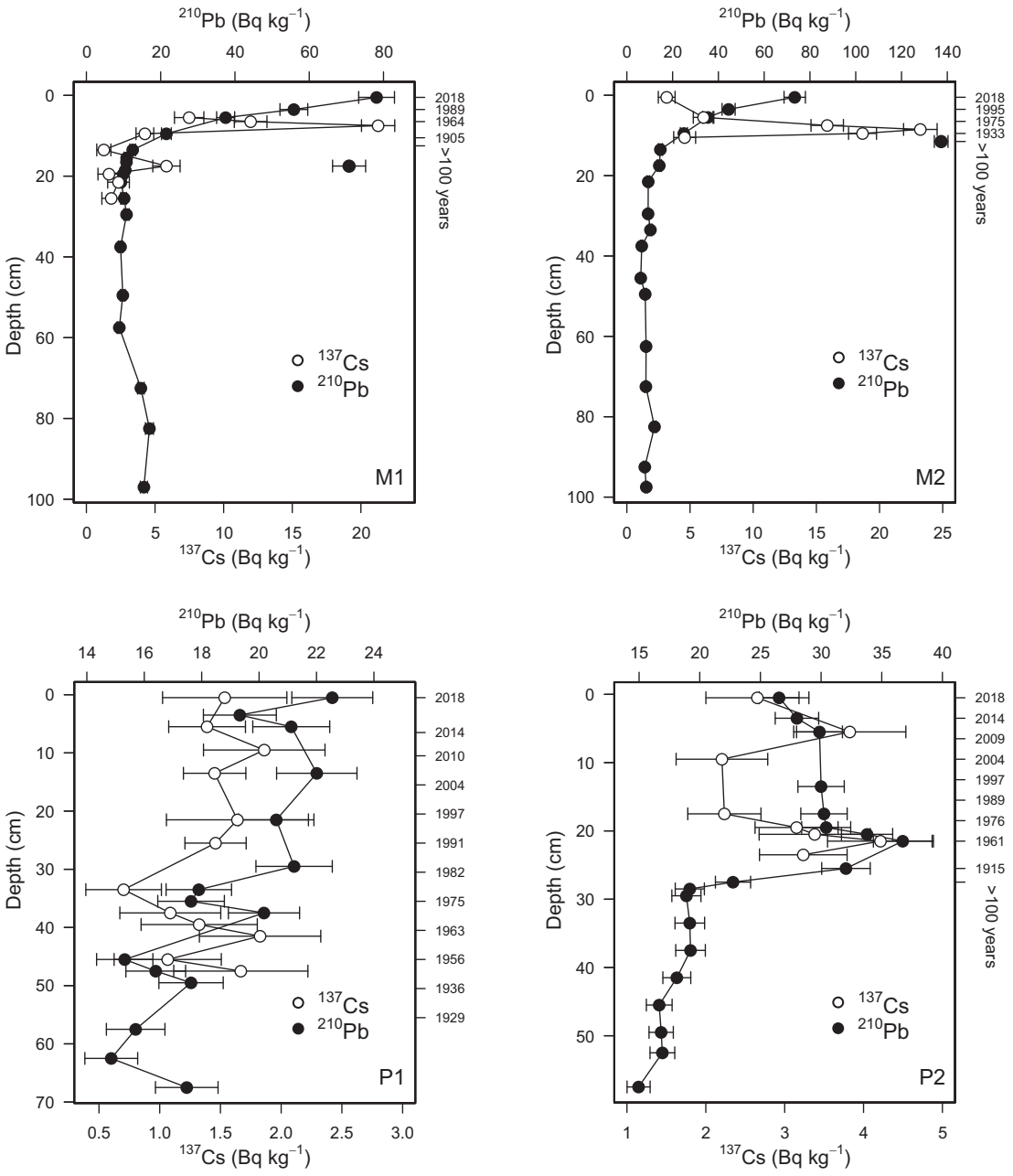

Fig. 2. Depth profile of $^{210}Pb_{total}$ and ^{137}Cs activities in sediment cores from San Quintín Bay, Mexican North Pacific.

3.2. Sediment characterization

The sediments were sand-silty (sand: 0.4–83.5%, silt: 14.8–91.1%) with low percentage of clays (1.6–15.1%, Fig. 4). The fine sediment (clay and silts) content in salt marsh cores was significantly ($p < 0.05$) higher than in seagrass cores, in which the sand content was significantly higher ($p < 0.05$) (Fig. 5). The grain size depth profiles showed almost constant values along the cores, excepting in the M2 core bottom, where sand content was higher (Fig. 4).

In core M1, the concentrations of Al, Zr, Ti, Ca, Sr and Mn decreased upwards, of Br, Na and Cl increased upwards and MS values showed lower values in the upper core segment (Fig. 4). Similarly, in the bottom segment of core M2 (67–100 cm), Al, Zr, Ti and MS decreased, and Br, Na and Cl increased upwards, but above this segment the profiles were erratic (Fig. 4). In P1, most elemental profiles were erratic. MS values increased from bottom to 41 cm, then decreased and displayed almost constant values from 27 cm to the surface. Br concentrations were constant from bottom to 41 cm and then decreased upwards, whereas the concentrations of Na and Cl increased upwards within in a small range (Fig. 4). In core P2, concentrations of Al, Zr, Ti, Mn showed greater variability than those of MS, Ca, Sr, Br, Na and Cl, which showed small variations. Some variables showed the lowest (Al, Zr and MS) or highest (Ca, Sr, Br, Na, Cl, C_{org} and N_{org}) values at mid-core (Fig. 4).

The concentrations of Al, Zr, Ti, MS, Ca, Sr and Mn were significantly higher, and Na, Cl, Br significantly lower, in seagrass than in salt marsh cores ($p < 0.05$, Fig. 5). However, all geochemical values were comparable ($p > 0.05$) between cores from each environment type, except Zr concentrations, which were significantly higher in P1 than in P2.

None of the C_{org} depth profiles showed an exponential decay caused by microbial degradation (Berner, 1964). In core M1, N_{org}, C_{inorg}, and C_{org} were almost constant from the bottom to 80 cm and increased upwards, whereas in core M2 increased upwards from the bottom to 46 cm and

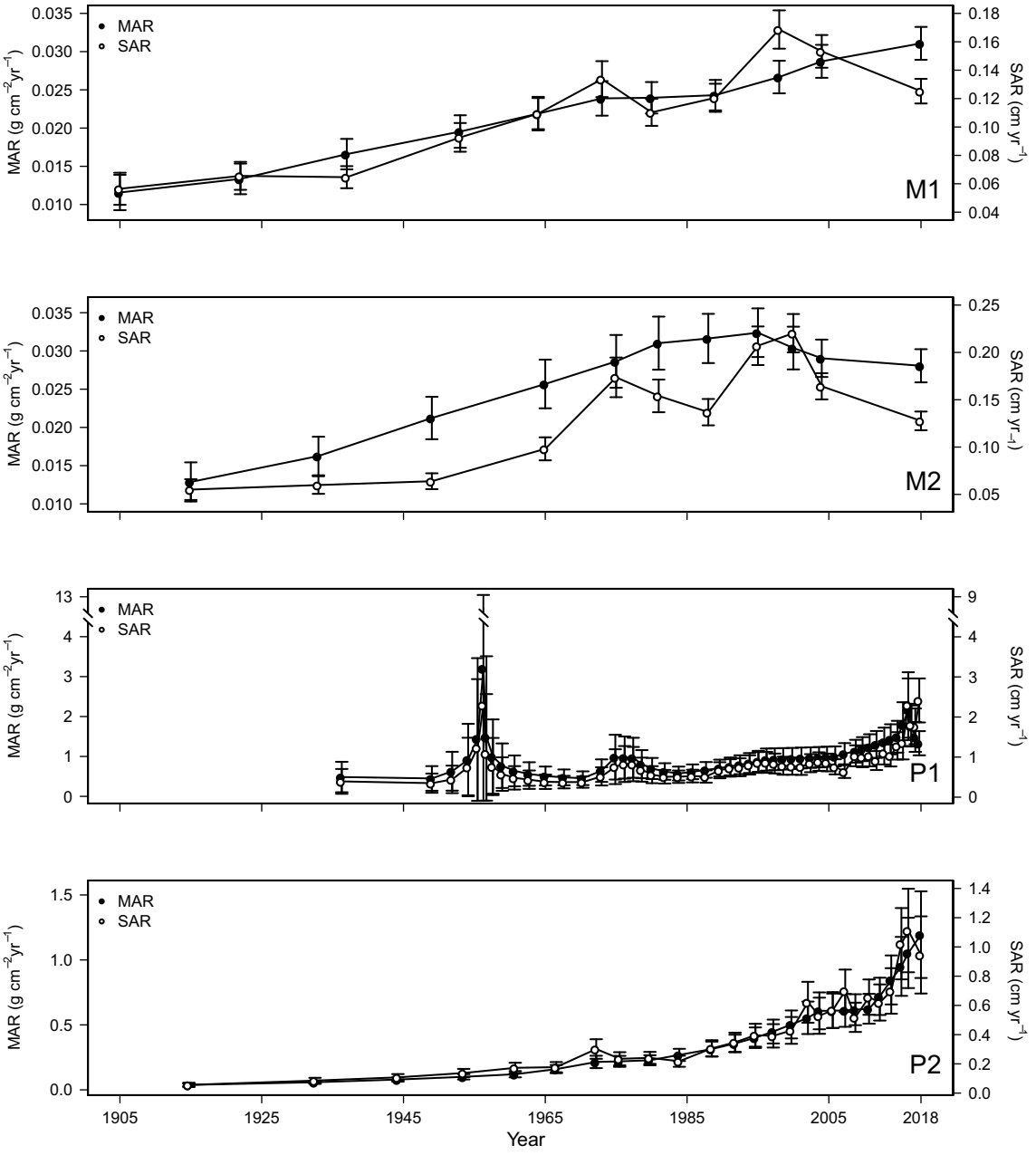

Fig. 3. Mass accumulation rate (MAR) and sediment accumulation rate (SAR) time evolution in cores from San Quintín Bay, Mexican North Pacific.

from there showed more variability. In the seagrass cores, N_{org} and C_{inorg} profiles showed maxima at mid-depth and C_{org} were almost constant from 50 cm to the core bottom. The concentrations of C_{org}, N_{org} and C_{inorg} in cores from each environment were comparable, but were significantly higher in salt marsh than in seagrass cores ($p < 0.05$, Fig. 5).

The C:N values were comparable among cores ($p > 0.05$), ranging from 10 to 21 in salt marsh cores and from 4 to 14 in seagrass cores. The C:N values were highest in the lowest segments of the salt marsh cores and in seagrass core P2, but varied erratically in core P1 (Fig. 4).

3.3. Factor analysis (FA)

According to FA, two factors explained 90% of the dataset variability. Factor 1 (F1, explained variance 52%) included as significant variables the concentrations of Al, Ti, Mn (positive loadings = 0.9) and Cl, C_{org}, Na, N_{org}, C_{inorg} and Br (negative loadings = −0.9 to −0.7). The significant variables of Factor 2 (F2, 38%) were silt and clay percentages (positive loadings = 0.9), and the sand percent and the concentrations of Zr, Sr and Ca (negative loadings = −0.9 to −0.7) (Fig. 6a). Salt marsh sediments spread along the F1 axis and grouped mostly on the positive side of the F2 axis, while seagrass sediments grouped only on the positive side of F1 axis and mostly on the negative side of F2 axis (Fig. 6b).

3.4. Organic carbon stocks and burial rates

The C_{org} stocks-$_{10cm}$ were comparable ($p > 0.05$) between cores at each environment type. In salt marsh cores the values ranged from 12.2 to 53.6 Mg ha^{-1}; and in both cores, a maximum value was observed between 40 and 50 cm depth (Fig. 7a) although this segment was out of the ^{210}Pb chronology. The C_{org} stocks-$_{10cm}$ (from surface to 50 cm) were significantly lower than those recorded below 50 cm. In

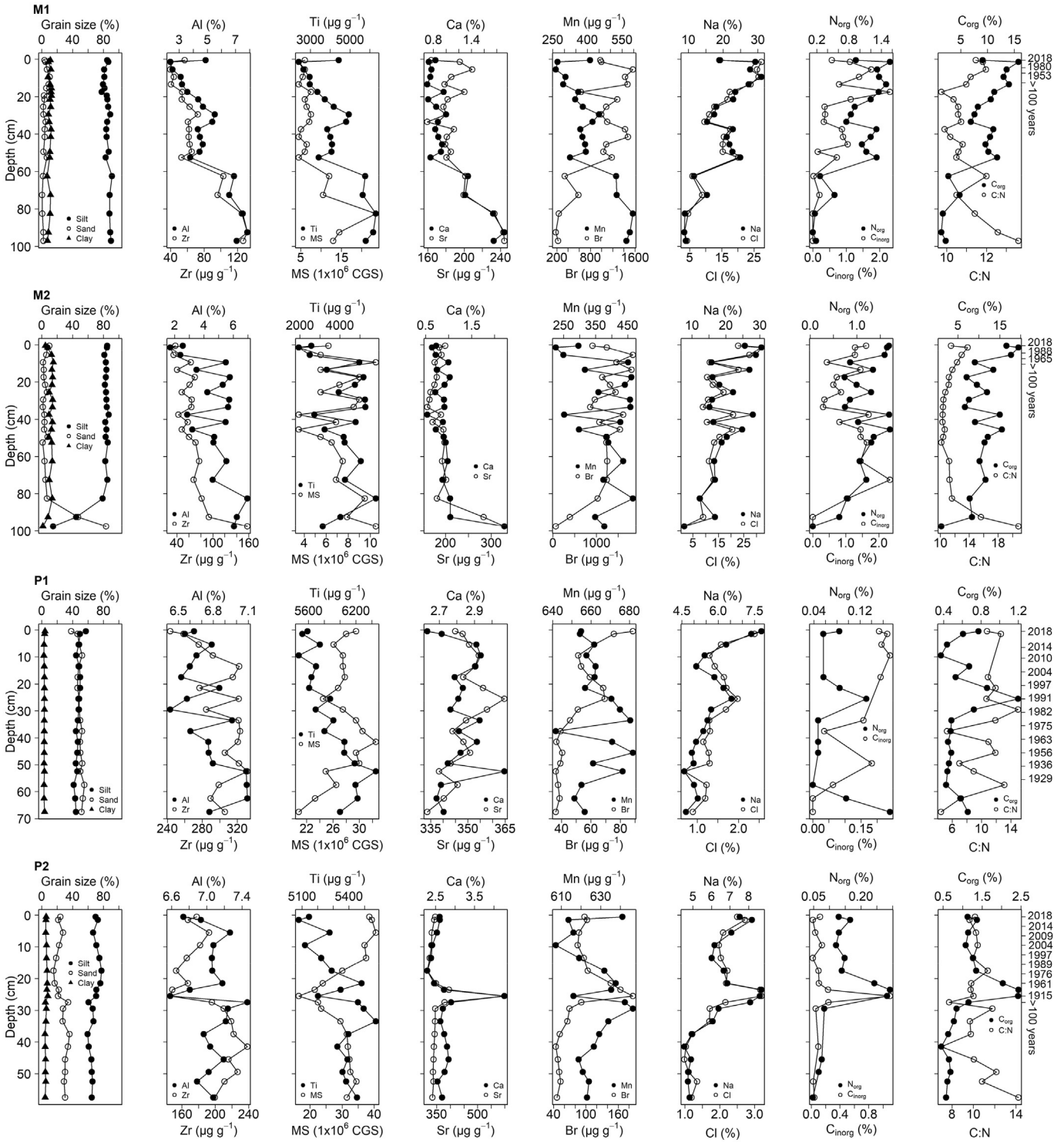

Fig. 4. Depth profiles of geochemical variables in seagrass and salt marsh sediment cores from San Quintín Bay, Mexican North Pacific.

the seagrass cores, the C_{org} stocks-$_{10cm}$ ranged from 5.7 to 14.4 Mg ha^{-1} and the values were rather homogeneous (Fig. 7a). The C_{org} stocks-$_{1m}$ were considerably higher in the salt marsh cores (259 ± 3 in M1, 320 ± 3 Mg ha^{-1} in M2) than in the seagrass cores (80 ± 3 in P1 and 98 ± 3 in P2 (Fig. 7b).

The C_{org} burial rate intervals were slightly higher in the salt marsh core M2 (13–60 g m^{-2} yr^{-1}) than M1 (15–45 g m^{-2} yr^{-1}), but similar in between the seagrass cores (P1: 20–114 g m^{-2} yr^{-1} -excluding the maxima between 1951 and 1960-, and in P2: 9–144 g m^{-2} yr^{-1}, Fig. 8). The C_{org} burial rates in both salt marsh cores and in P2 seagrass core showed a steady increase since last century and until the early 2000s (no defined trend was evident for P1). According to the slope of the regression analysis between C_{org} burial rates and time (from early 1900s to early 2000s, there was an increment rate between 0.29 and 0.64 g m^{-2} yr^{-1} per year within the salt marsh cores and 0.67 g m^{-2} yr^{-1} per year for core P2). On the other hand, since early 2000 to 2018 (sampling date), the C_{org} burial rate values decreased in the salt marshes, whereas in the seagrass cores, a considerable increment was observed (increment rates of 9.4 and 11.3 g m^{-2} yr^{-1} per year in P1 and P2 cores, respectively) (Fig. 8).

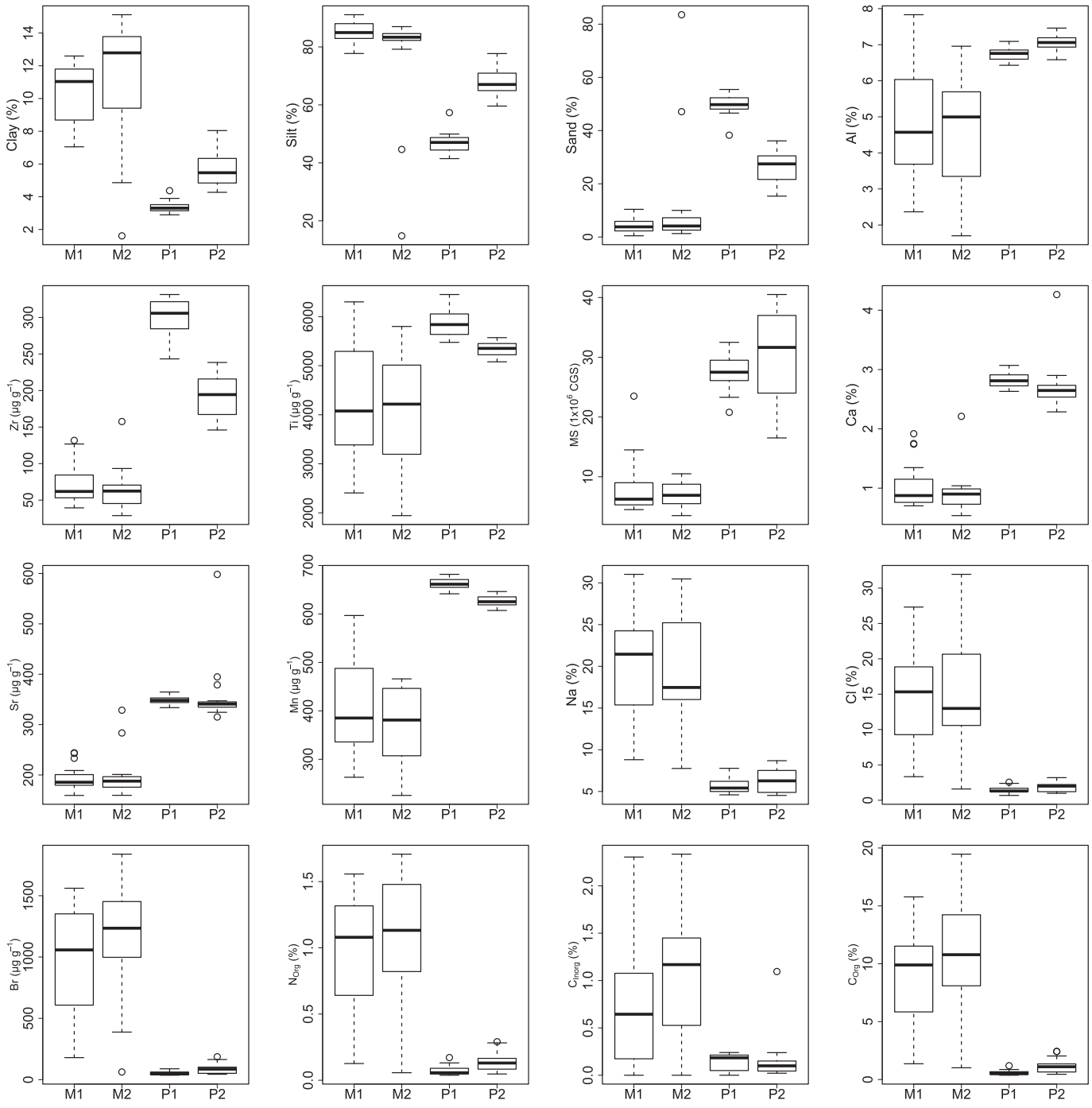

Fig. 5. Box-plot of geochemical variables that showed significant differences ($p < 0.05$) among seagrass and salt marsh cores from San Quintín Bay, Mexican North Pacific.

4. Discussion

4.1. Dating and sediment accumulation rates

$^{210}Pb_{xs}$ fluxes in salt marsh cores were lower than in seagrass cores (Table 1); and than the atmospheric flux predicted by Turekian et al. (1977) for Western North-America (~83 Bq m^{-2} yr^{-1}) but comparable with $^{210}Pb_{xs}$ fluxes estimated on the West coast of United States (25 ± 1.7 Bq m^{-2} yr^{-1} in Palo Alto and 35 ± 1.7 Bq m^{-2} yr^{-1} in Los Angeles (Fuller and Hammond, 1983). The lower $^{210}Pb_{xs}$ fluxes in SQB salt marshes is most likely the result of the low ^{210}Pb atmospheric flux in the eastern Mexican Pacific, attributed to the prevalence of shoreward winds with little $^{210}Pb_{ex}$ (Ruiz-Fernández and Hillaire-Marcel, 2009). The higher $^{210}Pb_{ex}$ fluxes in seagrass meadow cores are likely caused by preferential accumulation of sediments (sediment focusing) since the seagrass canopy in the water column acts as sediment trap (Mellors et al., 2002). Conversely, ^{137}Cs activities in salt marsh cores (≤0.3–18.5 Bq kg^{-1}) were higher than in seagrass cores (≤0.4–4.2 Bq kg^{-1}), resulting from (a) the direct atmospheric deposition, or deposition through runoff, of ^{137}Cs in the salt marsh, (b) the solubility of ^{137}Cs in seawater, causing lower deposition in seagrass sediments (Ruiz-Fernández and Hillaire-Marcel, 2009), and/or (c) the dilution of ^{137}Cs activities in seagrass cores owing to higher sediment accumulation.

The irregular ^{210}Pb profiles observed in seagrass cores (Fig. 2) are frequently attributed to mixing events, common in high energy areas where seagrass meadows develop. However, mixing would have produced homogenized profiles of other geochemical variables, which

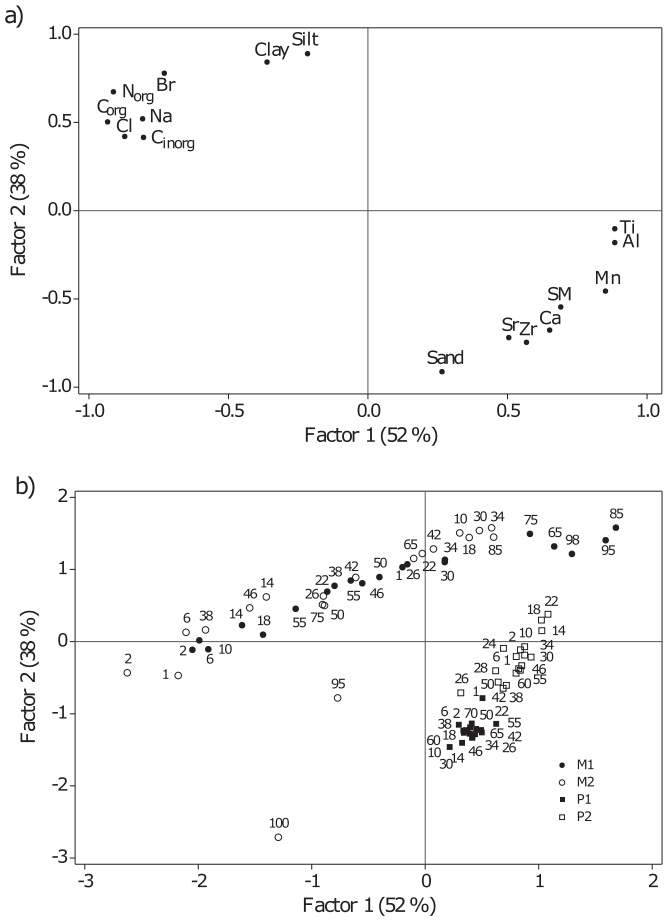

Fig. 6. Factor analysis of geochemical variables of sediment cores from San Quintín Bay, Mexican North Pacific, a) biplot and b) distribution of sediment samples.

was not the case (Fig. 4). Despite sediment resuspension events are possible, we considered that the irregular ^{210}Pb seagrass profiles were mainly the result of variable sediment supply. The low ^{210}Pb activities, recorded in the segments 42–47 cm (1951–1961) and 37–38 cm (1975–1982) in P1 (collected closer to the SQB mouth than P2 core), could have resulted from high sediment loads promoted by meteorological events in the area, such as the impact of hurricanes (unnamed in 1951 and 1959; Kathleen in 1976; NOAA, 2018a). Nonetheless, the ^{137}Cs depth profiles are in agreement with the ^{210}Pb-derived chronology.

Larger sediment accumulation in seagrass than in salt marsh cores was mostly caused by resuspension, transport of sediment by water currents and effective retention of suspended matter by the seagrass canopy. MAR in SQB salt marsh cores were lower than those reported for tropical salt marshes in Mexico, such as Estero de Urias, Gulf of California (0.03–0.15 g cm^{-2} yr^{-1}; Ruiz-Fernández et al., 2016), Salada Lagoon, Gulf of Mexico (0.03–0.88 g cm^{-2} yr^{-1}; Bojórquez-Sánchez et al., 2017) and Sian Ka'an, Mexican Caribbean Coast (0.06–0.28 g cm^{-2} yr^{-1}; Carnero-Bravo et al., 2016). They were also lower than in salt marshes of the western Arabian Gulf (0.40–0.94 g cm^{-2} yr^{-1}; Cusack et al., 2018) and tropical salt marshes in Jiquilisco Bay, El Salvador (0.07–0.52 g cm^{-2} yr^{-1}; Amaya-Monterrosa et al., 2014). SAR values in SQB salt marshes (0.06–0.22 cm yr^{-1}) fell within the range of most marshes worldwide (0.1–0.7 cm yr^{-1}; Alongi, 2018). For seagrass meadow cores, MAR were higher than seagrass meadows in Florida, USA (Big Lagoon: 0.59 ± 0.08 g cm^{-2} year^{-1}; Trevathan-Tackett et al., 2017b), western Arabian Gulf (0.08–0.34 g cm^{-2} year^{-1}; Cusack et al., 2018) and the Baltic Sea (0.24 ± 0.01 g cm^{-2} year^{-1}; Jankowska et al., 2016); and the SAR range was higher than the worldwide SAR interval of 0.06 to 0.6 cm yr^{-1} (Duarte et al., 2013).

4.2. Factor analysis

The association of terrigenous (Al, Ti and Mn) and marine (Na, Cl, Br) indicators elements in F1 identified this factor as *sediment provenance* (terrigenous vs. marine; Fig. 6a). In salt marsh cores, the marine signal (negative F1) has been increasing since >100 years ago (Fig. 6b), as confirmed by the upward increasing concentrations of marine indicator elements (Na, Cl, and Br, Fig. 4), most likely as a result of sea level rise, since larger periods of seawater inundation during higher tides induce salt accumulation in sediments (Shen et al., 2018). C_{org} was significantly correlated with N_{org} and C_{inorg} ($p < 0.05$) and were associated to marine indicators (negative F1), implying that higher C_{org} concentrations are favored by higher marine influence. This was confirmed by the C:N profiles (Fig. 4), which broadly showed an upward decreasing value, close to the values of marine-derived organic matter (C:N values ≤10; Parsons, 1975).

Factor 2, identified as *grain size distribution*, discriminated the energy of the sedimentary environment, and the C_{org} absorption capacity of the sediments. The highest sand content in seagrass sediments (Fig. 5) evidenced the strong hydrodynamics and explained the lowest C_{org} concentrations (Fig. 5) at this type of environment, since C_{org} content was mostly associated to the fine sediment contents ($p < 0.05$), implying that most C_{org} in seagrass sediments is sequestered from the water column by settling sediment particles. In contrast, despite salt marsh cores had the highest contents of fine sediments and C_{org} (Fig. 5), both variables were uncorrelated, most likely because of the C_{org} concentrations are the result of *in situ* production from surface vegetation and deposition (Turner et al., 2004).

The distribution of the sediment core sections in the FA biplot (Fig. 6b) showed that salt marsh sediments (spread along F1 and mostly with positive F2) are clearly distinct from seagrass sediments (positive F1 and mostly with negative F2). While seagrass sediments reflected a clear terrestrial influence, salt marsh sediments showed a transition from terrigenous to more marine conditions at present. The bottom sections of the salt marsh core M1 (and the bottom section of M2) showed

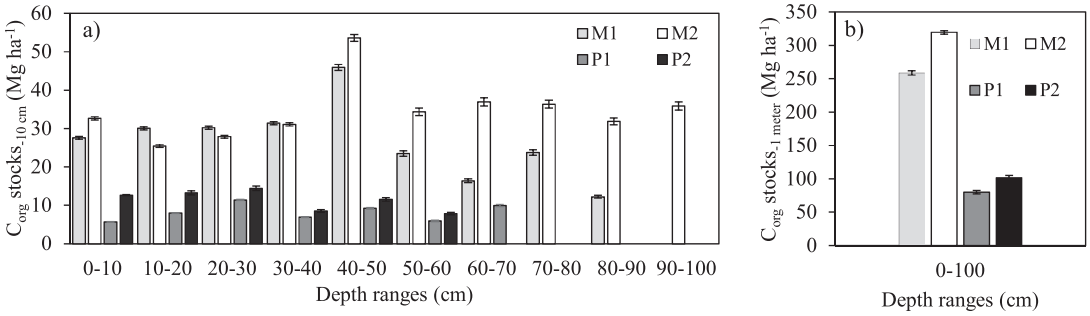

Fig. 7. C_{org} stocks in sediment cores from San Quintín Bay, Mexican North Pacific: a) C_{org} stocks-$_{10cm}$, b) C_{org} stocks-$_{1m}$.

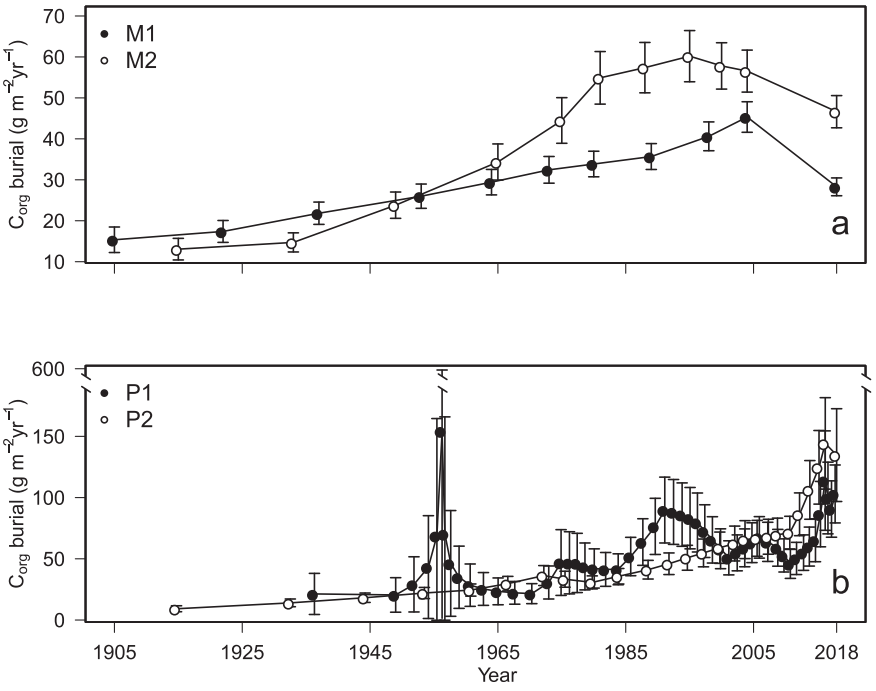

Fig. 8. Time evolution of C_{org} burial rates in (a) salt marsh and (b) seagrass cores from San Quintín Bay, Mexican North Pacific.

higher Al and Ti, and lower Na, Cl and Br that the uppermost sections, indicating the presence of a terrigenous environment with high C_{org} concentrations, very likely corresponding to the period before the establishment of the marsh pioneer species. Indeed, the marsh margins in SQB built out laterally over sands and sandy silts (Gorsline and Stewart, 1962) as reflected in the high sand contents of the bottom section of core M2. Once salt marsh pioneer species are established, they promote the settlement of sediment particles and the accumulation of organic material (Alongi, 2018), which would be in agreement with the overall increment of fine sediment, C_{org}, N_{org}, and C_{inorg} contents towards present in both cores (Fig. 4).

4.3. Carbon stocks and burial rates

The C_{org} stocks-$_{10cm}$ determined in seagrass and salt marsh cores since the last century were homogenous. However, in salt marsh cores maximum values were observed at 40–50 cm depth, which was out of the ^{210}Pb-dating range, and thus difficult to attribute its origin. Possible causes of this maximum stock could be related to changes in the marsh surface topography that influences the frequency and duration of flooding, tidal height, distribution of nutrients and suspended sediment (Kulawardhana et al., 2015 and references therein), higher marsh vegetation productivity owing to changes in environmental conditions, and/or changes in marsh species.

C_{org} stocks in the 50 cm upper segment in salt marsh cores (165.1–170.6 Mg ha^{-1}) were slightly higher than the mean C_{org} stock value for the top 50 cm in cores collected in the eastern SQB arm (146.0 Mg ha^{-1}, recalculated from Burke Watson and Hinojosa Corona, 2018). Although the variability in C_{org} stocks among different salt marshes have been partially explained by latitudinal differences (Ouyang and Lee, 2014), the salt marsh stocks in SQB cores at 1-meter depth (Table 2) were comparable to the global mean (317 ± 19 Mg C_{org} ha^{-1}; Alongi, 2018 and references therein). Our results also fell within the intervals estimated for tropical salt marshes in El Salvador, Gulf of California, and Mexican Caribbean coast (29.9–464.8 Mg ha^{-1}; Ruiz-Fernández et al., 2018) and in salt marshes from Australia (14.0–963.0 Mg ha^{-1}; Macreadie et al., 2017) (Table 2).

C_{org} storage depends on multiple biogeochemical and biotic factors that affect carbon production, import/export dynamics, and decomposition rates (Ouyang and Lee, 2014). C_{org} stocks-$_{1m}$ in SQB seagrass cores (Table 2) were lower than the global stock estimated for seagrass meadows (139.7 Mg C ha^{-1}; Fourqurean et al., 2012). In the case of *Z. marina* L., our stocks-$_{1m}$ were lower than those from the Mediterranean Sea (351.7 Mg ha^{-1}; Röhr et al., 2018), comparable to eastern and western Pacific (69.4 and 93.7 Mg ha^{-1}), slightly higher than in eastern and western Atlantic (55.4 and 54.0 Mg ha^{-1}) and ~4 fold higher than in the Baltic Sea (23.1 Mg ha^{-1}). The mud content in seagrass sediments from the Baltic sea (5.9 ± 0.8%; Röhr et al., 2018) is lower than that found in seagrass sediments from SQB (P1: 44%–62%; P2: 64%–85%), implying stronger hydrodynamic conditions in the Baltic Sea, causing lower C_{org} stocks.

Our results were also comparable with those obtained for seagrass meadows composed by *Halodule uninervis* (Forssk.) Asch., *Halophila stipulacae* (Forssk.) Asch. and *Halophila ovalis* (R. Br.) Hook f. in the western Arabian Gulf (76 ± 20 Mg ha^{-1}; Cusack et al., 2018), and by *Amphibolis antarctica* (Labill.) Asch. and *Posidonia australis* Hook.f. in Australia (128 ± 7 Mg ha^{-1}, Arias-Ortiz et al., 2018), but two times lower than *Thalassodendron ciliatum* (Forssk.) Hartog, *Thalassia hemprichii* (Ehrenb.) Asch., *Enhalus acoroides* (L.f.) Royle and *Syringodium isoetifolium* (Asch.) Dandy seagrass meadows in Kenya (236 ± 24 Mg ha^{-1}, Githaiga et al., 2017), and ~4 times lower than the stock in *Posidonia oceanica* (L.) Delile meadows in the Mediterranean (372.4 Mg ha^{-1}, Fourqurean et al., 2012) (Table 2).

The C_{org} stock differences among seagrass meadows composed by different species have been related with species characteristics and the environmental conditions in which they grow. For instance, highest C_{org} stocks are observed in continuous and high density meadows composed by large and persistent species with complex canopies (e.g. *Posidonia* spp. and *Thalassia* spp.), or by small and colonizer species (e.g. *Halophila* spp. and *Halodule* spp.) (Mazarrasa et al., 2018 and references therein). *Zostera marina* L. is the most abundant species in SQB meadows, and in most areas this species is found in high densities (Ward et al., 2003, 2004). *Zostera marina* L. is a fast-growing species and it is generally smaller than *Posidonia* spp., thus likely contributes less to the sediment organic matter (Dahl et al., 2016). In addition,

Table 2
C_{org} stock (Mg C_{org} ha^{-1}) at 1 m of depth in different seagrass and salt marshes environments.

Site	C_{org} stock (Mg C_{org} ha^{-1})	References
Salt marshes		
Australian coasts	14.0–963.0	Macreadie et al. (2017)
Salada Lagoon, Gulf of Mexico	115.6–130.7	Ruiz-Fernández et al. (2018)
Jiquilisco Bay, El Salvador	29.9–464.8	Ruiz-Fernández et al. (2018)
Estero de Urias Lagoon, Gulf of California, Mexico	305.3–362.0	Ruiz-Fernández et al. (2018)
Sian Ka'an, Mexican Caribbean coast	116.9–342.8	Ruiz-Fernández et al. (2018)
Zostera marina meadows		
Eastern and Western Pacific	69.4 and 93.7	Röhr et al. (2018)
Eastern and Western Atlantic	55.4 and 54.0	Röhr et al. (2018)
Baltic Sea	23.1	Röhr et al. (2018)
Mediterranean Sea	351.7	Röhr et al. (2018)
Meadows with dominance of other seagrass species		
Gazi Bay, Kenya	236 ± 24	Githaiga et al. (2017)
Shark Bay, Australia	128 ± 7	Arias-Ortiz et al. (2018)
Western Arabian Gulf	76 ± 20	Cusack et al. (2018)
Mediterranean Sea	372.4	Fourqurean et al. (2012)
San Quintín Bay, México:		
Seagrass cores	80 ± 3, 102 ± 4	This study
Salt marsh cores (western arm)	259 ± 3, 319 ± 3	This study

P. oceanica (L.) Delile organic remains (roots, rhizomes and leaves) form dense mats that contributes to greater C_{org} storage than other seagrass species (Mateo et al., 1997; Hori et al., 2019).

Likewise, the accumulation of C_{org} is promoted in shallow and sheltered environments with low energy and turbidity, and with low/mid nutrients inputs (Mazarrasa et al., 2018 and references therein). SQB is a shallow lagoon and the main hydrodynamic forces are tides and winds, which cause in the western arm large residual currents (Delgado-González et al., 2012; Melaku Canu et al., 2016) and turbulence (Jorgensen et al., 2007), that reduce C_{org} accumulation by sediment resuspension and export.

C_{org} stocks-$_{1m}$ for salt marsh cores were higher than for seagrass cores (Table 2), in agreement with Howard et al. (2014) and Alongi (2018). However, the maximum burial rates estimated for salt marsh cores (45–60 g m^{-2} $year^{-1}$) were lower than the maxima for seagrass cores: (114–144 g m^{-2} $year^{-1}$). This is clearly driven by the lower MAR in salt marsh habitat, which could be caused by a high exposure of salt marshes to winds, and a more efficient sedimentation in the seagrass meadows, which are located between the salt marsh areas and the lagoon connection to the sea, and may act as sediment sink, reducing the marine sediment flux to the salt marsh (Carr et al., 2018).

The increasing C_{org} burial rates in both salt marsh and seagrass cores through the last century were mostly driven by the small variations in MAR, which could be explained by the erosion promoted by land use changes, associated with a rapid human population growth and the economic development in the region. Agriculture activities in San Quintin Valley started since 1920s, peaked between 1980s and 1990s, and since 2000s, the installation of vast extensions of greenhouse cultivation areas (Rangel and Riemann, 2015) have promoted an outstanding economic growth during the last 15 years (SEFOA, 2015). On the other hand, the economic growth has promoted a rapid population increase (passing from 1000 inhabitants in 1950s to about 60,000 in 1996; Aguirre-Muñoz et al., 2001) necessarily associated with land cover changes owing to the expansion and multiplication of human settlements.

4.4. Salt marsh and seagrass meadows in the face of global change

Vegetated coastal ecosystems, which act as important C_{org} sinks, have an important role in climate change mitigation (Duarte et al., 2005, 2013; Alongi, 2018), but are also threatened by its impacts, such as sea-level rise, rainfall change, warming, and increasing storms frequency and intensity (Morzaria-Luna et al., 2014 and references therein), and by human impacts such as contamination and conversion into agriculture, industrial or urban developments (such as saltworks, mining, fishing, aquaculture, livestock grazing/trampling and siltation).

Bivalve aquaculture commonly occurs in intertidal zones, frequently overlapping with seagrass meadows and, in some cases, it can negatively affect seagrass density (Ferris et al., 2019). Also, physical disturbances associated with farming activities might reduce carbon sequestration owing to sediment destabilization (Barañano et al., 2018). However, oyster farming in the SQB western arm, developed since ~40 years ago, has not affected eelgrass density or coverage (Ward et al., 2003) and shoots exposed to oyster farming displayed higher vegetative production and photosynthetic rates (Sandoval-Gil et al., 2016). Indeed, no significant differences ($p > 0.05$) were observed for C_{org} stocks in seagrass cores before (P1: 1929–1976, 34–70 cm; P2: >100 years – 1975, 18–60 cm) and during the aquaculture period (P1: 1978–2018, surface – 33 cm; P2: 1979–2018, surface - 18 cm), confirming that the effects of aquaculture on C_{org} accumulation in these seagrass meadows are negligible, so far. It was not possible to evaluate the impact of the oyster aquaculture on salt marsh C_{org} stocks because of the low time resolution of the cores (the past 100 years are included in only 10 cm of sediment).

In SQB, warm temperatures observed during a strong El Niño event (1986–1987) were associated with the reduction of *Z. marina* L. growth rates (Echavarria-Heras et al., 2006), in agreement with the model simulations from Carr et al. (2012), showing their sensitivity to warming sea surface temperatures. Recent accretion of salt marshes in SQB is close to 1 mm yr^{-1}, lower than the mean global sea rise (3.0 ± 0.7 mm yr^{-1}; Hay et al., 2015) and than the relative sea level trend for the region (2.3 ± 1.4 mm yr^{-1}; NOAA, 2018b) which might imply that SQB salt marshes could not keep pace with recent sea level rise.

The overall stocks and recent burial rates of the two habitats were calculated by using their estimated total surface in 1999, with an uncertainty equal to half the error of commission (reported in Ward et al., 2004), and the mean values of C_{org} stocks-$_{1m}$ and surface burial rates for each habitat (Table 1). The overall C_{org} stock in salt marshes (283 ± 39 Gg) was significantly ($p < 0.05$) larger than in seagrasses (202 ± 32 Gg), owing to the larger C_{org} concentrations in salt marsh sediments. The overall C_{org} stock of both habitats together (485 ± 51 Gg C) is 1.2 times larger than the one year net C emissions in the nearby city of Ensenada in 2005 (400 Gg C; Bullock et al., 2011). Contrarily, the recent burial rate in salt marshes (0.367 ± 0.12 Gg yr^{-1}) was significantly smaller ($p < 0.05$) than in seagrasses (2.6 ± 0.9 Gg yr^{-1}), mainly owing to lower MAR of salt marshes. In total, both habitats bury carbon at a rate of 3.0 ± 0.9 Gg yr^{-1}, about 28% of the estimated net C annual emissions of the nearby town of San Quintín, assuming a per capita C emission rate similar to inhabitants of Ensenada. We therefore concluded that both habitats play a relevant role as carbon sinks.

5. Conclusions

The 100 year temporal variations of C_{org} stocks and burial rates were evaluated in ^{210}Pb-dated sediment cores from seagrass and salt marsh areas in San Quintín Bay. The C_{org} stocks-$_{10cm}$ were comparable in each habitat but different between them. The C_{org} stocks-$_{1m}$ in salt marsh were also higher than in seagrass cores, mostly owing to *in situ* production and the prevalence of fine particles in salt marshes, which are very effective to absorb C_{org}. The C_{org} stock values obtained from the salt marsh were within the global ranges reported in the literature and the C_{org} stocks in seagrass sediment cores were lower than the

global ranges, but comparable with regional values from the Eastern and Western Pacific. The recent C_{org} burial rates were larger in seagrass than in salt marsh cores and their temporal changes were mostly driven by variations in accumulation rates, resulting from land use changes in the surroundings.

No evidence was found that anthropogenic activities developed within and around the western arm of SQB have impacted the C_{org} stocks in the seagrass meadows areas. Assuming homogenous behavior of both habitats for C_{org} dynamics, the total 1 m C_{org} stock is larger in salt marshes than in seagrasses, and the opposite for the total burial rates. The total 1 m C_{org} stock is larger to one year of net C emissions in the city of Ensenada, and the total burial rates is smaller but of the same order of magnitude than the net annual C emissions in the nearby town of San Quintín.

Salt marshes and seagrass meadows are efficient carbon sinks, but their resilience to global change is not unlimited. Their management and protection are effective strategies to mitigate climate change. It is therefore urgent to design and implement management measures to protect these habitats.

Acknowledgements

This work was supported by the grant CONACYT PDCPN 2015/1-473. The authors thanks H. Bojórquez-Leyva and S. Rendón-Rodríguez for technical assistance, and E. Cruz-Acevedo, G. Ramírez-Reséndiz and C. Suárez, for data management.

References

Aguirre-Muñoz, A., Buddemeier, R.W., Camacho-Ibar, V.F., Carriquiry, J.D., Ibarra-Obando, S.E., Massey, B.W., Smith, S.V., Wulff, F., 2001. Sustainability of coastal resource use in San Quintin, Mexico. Ambio 30, 142–149. https://doi.org/10.1579/0044-7447-30.3.142.

Alongi, D.M., 2018. Blue carbon coastal sequestration for climate change mitigation. Springer Briefs in Climate Studies. Australia 88.

Álvarez-Borrego, S., 2004. Nutrient and phytoplankton dynamics in a coastal lagoon strongly affected by coastal upwelling. Cienc. Mar. 30 (1A), 1–19. https://doi.org/10.7773/cm.v30i1A.2510.

Amaya-Monterrosa, O.A., Machain-Castillo, M.L., Ruiz-Fernández, A.C., Sanchez-Cabeza, J.A., Carranza-Edwards, A., Cearreta, A., Cabrera-Ramírez, M.A., Espinoza-Navarrete, J., Meza-Guerrero, E., Perez-Bernal, L.H., Rodriguez-Ramirez, A., 2014. Geochemical and micropaleontological evidence of recent hydrological changes in sedimentary records of Jiquilisco Bay, El Salvador. Cienc. Mar. 40 (4), 305–320. https://doi.org/10.7773/cm.v40i4.2475.

Arellano-Méndez, L., Morales-Ojeda, S., Herrera-Silveira, J. 2015. Carbono orgánico de las praderas de *Thalassia testudinum* en Bahía de la Ascensión (Quintana Roo, México). Una primera estimación del contenido de carbono azul en una laguna costera del Caribe Mexicano. In: Paz, F., Wong, J., (Eds). Estado Actual del Conocimiento del Ciclo del Carbono y sus Interacciones en México: Síntesis a 2014. Serie Síntesis Nacionales. Programa Mexicano del Carbono en colaboración con el Centro de Investigación y Estudios Avanzados del Instituto Politécnico Nacional, Unidad Mérida y el Centro de Investigación y Asistencia en Tecnología y Diseño del Estado de Jalisco. Texcoco, Estado de México, México. 421–427.

Arellano-Méndez, L.U., Bello-Pineda, J., Aké-Castillo, J.A., Pérez-España, H., Martinez-Cardenas, L., 2016. Distribución espacial y estructura morfométrica de las praderas de *Thalassia testudinum* (Hydrocharitaceae) en dos arrecifes del Parque Nacional Sistema Arrecifal Veracruzano. México. Rev. Biol. Trop. 64 (2), 427–448.

Arias-Ortiz, A., Serrano, O., Masqué, P., Lavery, P.S., Mueller, U., Kendrick, G.A., Rozaimi, M., Esteban, A., Fourqurean, J.W., Marbà, N., Mateo, M.A., Murray, K., Rule, M.J., Duarte, C.M., 2018. A marine heatwave drives massive losses from the world's largest seagrass carbon stocks. Nat. Clim. Chang. 8, 338–344. https://doi.org/10.1038/s41558-018-0096-y.

Ávila-López, M.C., Hernández-Ayón, M., Camacho-Ibar, V.F., Bermúdez, A.F., Mejía-Trejo, A., Pacheco-Ruiz, I., Sandoval-Gil, J.M., 2017. Air–water CO2 fluxes and net ecosystem production changes in a Baja California coastal lagoon during the anomalous North Pacific warm condition. Estuar. Coasts 40 (3), 792–806. https://doi.org/10.1007/s12237-016-0178-x.

Barañano, C., Fernández, E., Méndez, G., 2018. Clam harvesting decreases the sedimentary carbon stock of a *Zostera marina*. Aquat. Bot. 146, 48–57. https://doi.org/10.1016/j.aquabot.2017.12.002.

Berner, R.A., 1964. An idealized model of dissolved sulfate distribution in recent sediments. Geochim. Cosmochim. Acta 28, 1497–1503.

Bojórquez-Sánchez, S., Marmolejo-Rodríguez, A.J., Ruiz-Fernández, A.C., Sánchez-González, A., Sánchez-Cabeza, J.A., Bojórquez-Leyva, H., Pérez-Bernal, L.H., 2017. Trace element fluxes during the last 100 years in sediment near a nuclear power plant. Estuar. Coast. Shelf Sci. 198, 343–353. https://doi.org/10.1016/j.ecss.2017.05.005 Part B.

Bullock, S.H., Escoto-Rodríguez, M., Smith, S.V., Hinojosa, A., 2011. Carbon flux of an urban system in México. J. Ind. Ecol. 15 (4), 512–526. https://doi.org/10.1111/j.1530-9290.2011.00341.x.

Burke Watson, E., Hinojosa Corona, A., 2018. Assessment of blue carbon storage by Baja California (Mexico) tidal wetlands and evidence for wetland stability in the face of anthropogenic and climatic impacts. Sensors 18 (32), 1–17. https://doi.org/10.3390/s18010032.

Carnero-Bravo, V., Sanchez-Cabeza, J.A., Ruiz-Fernández, A.C., Merino-Ibarra, M., Hillaire-Marcel, C., Corcho-Alvarado, J.A., Zavala-Hidalgo, J., 2016. Sedimentary records of recent sea level rise and acceleration in the Yucatan Peninsula. Sci. Total Environ. 573, 1063–1069. https://doi.org/10.1016/j.scitotenv.2016.08.142.

Carnero-Bravo, V., Sanchez-Cabeza, J.A., Ruiz-Fernández, A.C., Merino-Ibarra, M., Corcho-Alvarado, J.A., Sahlie, H., Hélief, J.F., Preda, M., Zavala-Hidalgo, J., Díaz-Asencio, M., Hillaire-Marcel, C., 2018. Sea level rise sedimentary record and organic carbon fluxes in a low-lying tropical coastal ecosystem. Catena 162, 421–430. https://doi.org/10.1016/j.catena.2017.09.016.

Carr, J.A., D'Odorico, P., McGlathery, K.J., Wiberg, P.L., 2012. Modeling the effects of climate change on eelgrass stability and resilience: future scenarios and leading indicators of collapse. Mar. Ecol. Prog. Ser. 448, 289–301. https://doi.org/10.3354/meps09556.

Carr, J., Mariotti, G., Fahgerazzi, S., McGlathery, K., Wiberg, P., 2018. Exploring the impacts of seagrass on coupled marsh-tidal flat morphodynamics. Front. Environ. Sci. 6, 92. https://doi.org/10.3389/fenvs.2018.00092.

CEC, 2016. North America's Blue Carbon: Assessing Seagrass, Salt Marsh and Mangrove Distribution and Carbon Sinks. Montreal, Canada: Commission for Environmental Co-operation. 54.

Chmura, G.L., Anisfeld, S.C., Cahoon, D.R., Lynch, J.C., 2003. Global carbon sequestration in tidal, saline wetland soils. Glob. Biogeochem. Cycles 17, 1111. https://doi.org/10.1029/2002GB001917.

CONABIO, 2013. Comisión Nacional para el Conocimiento y Uso de la Biodiversidad. Distribución de los manglares en México en 2010. Available at: https://www.biodiversidad.gob.mx/ecosistemas/manglares2013/extensionDist.html. Accessed on: 01/19/2018.

Cusack, M., Saderne, V., Arias-Ortiz, A., Masqué, P., Krishnakumar, P.K., Rabaoui, L., Qurban, M.A., Qasem, A.M., Prihartato, P., Loughland, R.A., Elyas, A.A., Duarte, C.M., 2018. Organic carbon sequestration and storage in vegetated coastal habitats along the western coast of the Arabian Gulf. Environ. Res. Lett. 13, 074007. https://doi.org/10.1088/1748-9326/aac899.

Daesslé, L.W., Rendón-Márquez, G., Camacho-Ibar, V.F., Gutiérrez- Galindo, E.A., Shumilin, E., Ortiz-Campos, E., 2009. Geochemistry of modern sediments from San Quintín coastal lagoon, Baja California: implications for provenance. Rev. Mex. Cienc. Geol. 26, 117–132.

Dahl, M., Deyanova, D., Gütschow, S., Asplund, M.E., Lyimo, L.D., Karamfilov, V., Santos, R., Björk, M., Gullström, M., 2016. Sediment properties as important predictors of carbon storage in *Zostera marina* meadows: a comparison of four European areas. PLoS One 11 (12), e0167493. https://doi.org/10.1371/journal.pone.0167493.

Delgado-González, O., Marván-Gargollo, F., Mejía-Trejo, A., Gil-Silva, E., 2012. San Quintin Lagoon hydrodynamics case study. Water Resources Management and Modeling. In: Nayak, P., (Ed.). InTech. Available from: http://www.intechopen.com/books/water-resourcesmanagement-and-modeling/san-quintin-lagoon-hidrodynamics-case-study. Accessed on: 11/07/2018.

Duarte, C.M., 2002. The future of seagrass meadows. Environ. Concerv. 29 (2), 192–206. https://doi.org/10.1017/S0376892902000127.

Duarte, C.M., Middelburg, J., Caraco, N., 2005. Major role of marine vegetation on the oceanic carbon cycle. Biogeosciences 2, 1–8. https://doi.org/10.5194/bg-2-1-2005.

Duarte, C.M., Losada, I.J., Hendriks, I.E., Mazarrasa, I., Marba, N., 2013. The role of coastal plant communities for climate change mitigation and adaptation. Nat. Clim. Chang. 3, 961–968. https://doi.org/10.1038/nclimate1970doi:10.1038/nclimate1970.

Echavarria-Heras, H.A., Solana-Arellano, E., Franco-Vizcaino, E., 2006. The role of increased sea surface temperature on eelgrass leaf dynamics: onset of El Niño as a proxy for global climate change in San Quintín Bay, Baja California. Bull. Southern California Acad. Sci. 105 (3), 113–127. https://doi.org/10.3160/0038-3872(2006)105[113:TROISS]2.0.CO;2.

Ferris, E.B., Conway-Cranos, L.L., Sanderson, B.L., Hoberecht, L., 2019. Bivalve aquaculture and eelgrass: a global meta-analysis. Aquaculture 498, 25–262. https://doi.org/10.1016/j.aquaculture.2018.08046.

Fourqurean, J.W., Duarte, C.M., Kennedy, H., Marbà, N., Holmer, M., Mateo, M.A., Apostolaki, E.T., Kendrick, G.A., Krause-Jensen, D., Mcglathery, K.J., 2012. Seagrass ecosystems as a globally significant carbon stock. Nat. Geosci. 5, 505–509. https://doi.org/10.1038/ngeo1477.

Fuller, C., Hammond, D.E., 1983. The fallout rate of ^{210}Pb on the western coast of United States. Geophys. Res. Lett. 10 (12), 1164–1167. https://doi.org/10.1029/GL010i012p01164.

García-Esquivel, Z., González-Gómez, M.A., Ley-Lou, F., Mejía-Trejo, A., 2004. Oyster culture potential in the west arm of San Quintín Bay: current biomass and preliminary estimate of the carrying capacity. Cien. Mar. 30 (1A), 61–74.

Gedan, K.B., Silliman, B.R., Bertness, M.D., 2009. Centuries of human-driven change in salt marsh ecosystems. Annu. Rev. Mar. Sci. 1 (1), 117–141. https://doi.org/10.1146/annurev.marine.010908.163930.

Githaiga, M.N., Kairo, J.G., Gilpin, L., Huxham, M., 2017. Carbon storage in the seagrass meadows of Gazi Bay, Kenya. PLoS One 12 (5), e0177001. https://doi.org/10.1371/journal.pone.0177001.

Gorsline, D.S., Stewart, R.A., 1962. Benthic marine exploration of Bahia de San Quintin, Baja California, 1960–61. Marine and Quaternary geology. Pac. Nat. 2, 281–319.

Hay, C.C., Morrow, E., Kopp, R.E., Mitrovica, J.X., 2015. Probabilistic reanalysis of twentieth-century sea-level rise. Nature 517 (7535), 481.

Hori, M., Bayne, C.J., Kuwae, T., 2019. Blue Carbon: characteristics of the ocean's sequestration and storage ability of carbon dioxide. In: Kuwae, T., Hori, M. (Eds.), Blue Carbon

in Shallow Coastal Ecosystems Carbon Dynamics, Policy, and Implementation. Springer, Singapore (1–31 pp.).
Howard, J., Isensee, K., Kennedy, H., Pidgeon, E., Telszewski, M., Crooks, S., Emmer, I., Herr, D., Hoyt, S., Laffoley, D., Quesada, M., Wagey, T., 2014. Why measure carbon stocks. In Howard, J., Hoyt, S., Isensee, K., Pidgeon, E., Telszewski, M. (eds.), Coastal Blue Carbon: Methods for Assessing Carbon Stocks and Emissions Factors in Mangroves, Tidal Salt Marshes, and Seagrass Meadows. Conservation International, Intergovernmental, Oceanographic Commission of UNESCO, International Union for Conservation of Nature. Arlington, Virginia, USA. 15–24.
Huxham, M., Whitlock, D., Githaiga, M., Dencer-Brown, A., 2018. Carbon in the coastal seascape: how interactions between mangrove forests, seagrass meadows and tidal marshes influence carbon storage. Curr. For. Rep. 4 (2), 101–110. https://doi.org/10.1007/s40725-018-0077-4.
Ibarra-Obando, S.E., Camacho-Ibar, V.F., Carriquiry, J.D., Smith, S.V., 2001. Upwelling and lagoonal ecosystems of the dry Pacific coast of Baja California. In: Seeliger, U., Kjerfve, B., (eds.), Coastal Marine Ecosystems of Latin America. Springer-Verlag Berlin Heidelberg. Ecological. Studies 144 (315–330 pp.).
Ibarra-Obando, S.E., Smith, S.V., Poumian-Tapia, M., Camacho-Ibar, V., Carriquiry, J.D., Montes-Hugo, M., 2004. Benthic metabolism in San Quintín Bay, Baja California, Mexico. Mar. Ecol. Prog. Ser. 283, 99–112. https://doi.org/10.3354/meps283099.
Jankowska, E., Michel, L.N., Zaborska, A., Włodarska-Kowalczuk, M., 2016. Sediment carbon sink in low-density temperate eelgrass meadows (Baltic Sea). J. Geophys. Res. Biogeosci. 121. https://doi.org/10.1002/2016JG003424.
Jorgensen, P., Ibarra-Obando, S.E., Carriquiry, J.D., 2007. Top-down and bottom-up stabilizing mechanisms in eelgrass meadows differentially affected by coastal upwelling. Mar. Ecol. Prog. Ser. 333, 81–93. https://doi.org/10.3354/meps333081.
Jorgensen, P., Ibarra-Obando, S.E., Carriquiry, J.D., 2010. Management of natural Ulva spp. blooms in San Quintin Bay, Baja California: is it justified? J. Appl. Phycol. 22, 549–558. https://doi.org/10.1007/s10811-009-9491-0.
Kulawardhana, R.W., Feagin, R.A., Popescu, S.C., Boutton, T.W., Yeager, K.M., Bianchi, T.S., 2015. The role of elevation, relative sea-level history and vegetation transition in determining carbon distribution in *Spartina alterniflora* dominated salt marshes. Estuar. Coast. Shelf Sci. 154 (2015), 48–57. https://doi.org/10.1016/j.ecss.2014.12.032.
Li, X., Bellerby, R., Craft, C., Widney, S.E., 2018. Coastal wetland loss, consequences, and challenges for restoration. Anthropocene Coasts, 1:1–15 https://doi.org/10.1139/anc-2017-0001.
Macreadie, P.I., Ollivier, Q.R., Kelleway, J.J., Serrano, O., Carnell, P.E., Lewis, C.J.E., Atwood, T.B., Sanderman, J., Baldock, J., Connolly, R.M., Duarte, C.M., Lavery, P.S., Steven, A., Lovelock, C.E., 2017. Carbon sequestration by Australian tidal marshes. Sci. Rep. 7, 44071. https://doi.org/10.1038/srep44071.
Martínez-Ríos, L., 2007. Ficha informática Ramsar Bahía de San Quintín, Baja Califronia, México. Servicio de información sobre sitios Ramsar. Available at https://rsis.ramsar.org/es/ris/1775 on 19/29/2018.
Mateo, M.A., Romero, J., Pérez, M., Littler, M.M., Littler, D.S., 1997. Dynamics of millenary organic deposits resulting from growth of the Mediterranean seagrass *Posidonia oceanica*. Est. Coast. Shelf. Sci. 44, 103–110.
Mazarrasa, I., Samper-Villareal, J., Serrano, O., Lavery, P.S., Lovelock, C.E., Marbà, N., Duarte, C.M., Cortés, J., 2018. Habitat characteristics provide insights of carbon storage in seagrass meadows. Mar. Poll. Bull. 134, 106–117. https://doi.org/10.1016/j.marpolbul.2018.01.059.
Mcleod, E., Chmura, G.L., Bouillon, S., Salm, R., Björk, M., Duarte, C.M., Lovelock, C.E., Schlesinger, W.H., Silliman, B.R., 2011. A blueprint for blue carbon: toward an improved understanding of the role of vegetated coastal habitats in sequestering CO2. Front. Ecol. Environ. 7, 362–370. https://doi.org/10.1890/110004.
Mcowen, C., Weatherdon, L.V., Van Bochove, J.W., Sullivan, E., Blyth, S., Zockler, C., Stanwell-Smith, D., Kingston, N., Martin, C., Spalding, M., Fletcher, S., 2017. A global map of salt marshes. Biodivers. Data J. 5, e11764. https://doi.org/10.3897/BDJ.5.e11764.
Melaku Canu, D., Aveytua-Alcázar, L., Camacho-Ibar, V.F., Querin, S., Solidoro, C., 2016. Hydrodynamic properties of San Quintin Bay, Baja California: merging models and observations. Mar. Poll. Bull. 108, 203–214. https://doi.org/10.1016/j.marpolbul.2016.04.030.
Mellors, J., Marsh, H., Carruthers, T.J.B., Waycott, M., 2002. Testing the sediment-trapping paradigm of seagrass: do seagrasses influence nutrient status and sediment structure in tropical intertidal environments? Bull. Mar. Sci. 71 (3), 1215–1226.
Morzaria-Luna, H., Turk-Boyer, P., Rosemartin, A., Camacho-Ibar, V.F., 2014. Vulnerability to climate change of hypersaline salt marshes in the Northern Gulf of California. Ocean Coast. Manage. 93, 37–50. https://doi.org/10.1016/j.ocecoaman.2014.03.004.
NOAA, National Oceanic and Atmospheric Administration U.S., 2018a. Historical hurricane tracks. Available from: https://coast.noaa.gov/hurricanes/. Accessed on: 12/14/2018.
NOAA, National Oceanic and Atmospheric Administration U.S., 2018b. Relative sea level trend (830-001 Ensenada, Mexico; mean sea level data from 1956 to 1990). Available from: https://tidesandcurrents.noaa.gov/sltrends/sltrends_station.shtml?id=830-001. Accessed on: 22/01/2019.
Ouyang, X., Lee, S.Y., 2014. Updated estimates of carbon accumulation rates in coastal marsh sediments. Biogeosciences 11, 5057–5071. https://doi.org/10.5194/bg-11-1-2014.
Parsons, T.R., 1975. Particulate organic carbon in the sea. In: Skirrow, G. (Ed.), Chemical Oceanography Riley, J. P. Academie Press, London, pp. 338–425.
Pendleton, L., Donato, D., Murray, B.C., Crooks, S., Jenkins, W.A., Sifleet, S., et al., 2012. Estimating global "blue carbon" emissions from conversion and degradation of vegetated coastal ecosystems. PLoS One 7, e43542. https://doi.org/10.1371/journal.pone.0043542.
Rangel, N., Riemann, H., 2015. Los humedales en la región Camalú-El Rosario: de las misiones a la agricultura en el valle de San Quintín. In Riemann, H., (Ed). El agua en la región agrícola Camalú-El Rosario, Baja California Un recurso sobreexplotado con repercusiones sociales y ambientales. Red Nacional de Investigación Urbana, Mexico. 29–56.
Röhr, M.E., Holmer, M., Baum, J.K., Björk, M., Chin, D., Chalifour, L., et al., 2018. Blue carbon storage capacity of temperate eelgrass (*Zostera marina*) meadows. Glob. Biogeochem. Cycles 32, 1–18. https://doi.org/10.1029/2018GB005941.
Ruiz-Fernández, A.C., Hillaire-Marcel, C., 2009. ^{210}Pb-derived ages for the reconstruction of terrestrial contaminant history into the Mexican Pacific coast: potential and limitations. Mar. Pollut. Bull. 59 (4), 134–145. https://doi.org/10.1016/j.marpolbul.2009.05.006.
Ruiz-Fernández, A.C., Sanchez-Cabeza, J.A., Serrato de la Peña, J.L., Perez-Bernal, L.H., Cearreta, A., Flores-Verdugo, F., Machain-Castillo, M.L., Chamizo, E., García-Tenorio, R., Queralt, I., Dunbar, R., Mucciarone, D., Diaz-Asencio, M., 2016. Accretion rates in coastal wetlands of the southeastern Gulf of California and their relationship with sea-level rise. The Holocene 26 (7), 1126–1137. https://doi.org/10.1177/0959683616632882.
Ruiz-Fernández, A.C., Carnero-Bravo, A., Sanchez-Cabeza, J.A., Pérez-Bernal, L.H., Amaya-Monterrosa, O.A., Bojórquez-Sánchez, S., López-Mendoza, P.G., Cardoso-Mohedano, J.G., Dunbar, R.B., Mucciarone, D.A., Marmolejo-Rodríguez, A.J., 2018. Carbon burial and storage in tropical salt marshes under the influence of sea level rise. Sci. Tot. Environ. 630, 1628–1640. https://doi.org/10.1016/j.scitotenv.2018.02.246.
Sanchez-Cabeza, J.A., Ruiz-Fernández, A.C., 2012. ^{210}Pb sediment radiochronology: an integrated formulation and classification of dating models. Geochim. Cosmochim. Acta 82, 183–200. https://doi.org/10.1016/j.gca.2010.12.024.
Sanchez-Cabeza, J.A., Ruiz-Fernández, A.C., Ontiveros-Cuadras, J.F., Bernal, L.H.P., Olid, C., 2014. Monte Carlo uncertainty calculation of ^{210}Pb chronologies and accumulation rates of sediments and peat bogs. Quat. Geochronol. 23, 80–93. https://doi.org/10.1016/j.quageo.2014.06.002.
Sandoval-Gil, J., Alexandre, A., Santos, R., Camacho-Ibar, V.F., 2016. Nitrogen uptake and internal recycling in *Zostera marina* exposed to oyster farming: eelgrass potential as a natural biofilter. Estuar. Coasts 39, 1694–1708. https://doi.org/10.1007/s12237-016-0102-4.
SEFOA, 2015. Panorama general de "zona San Quintín" Baja California. Secretaría de Fomento Agropecuario. Available from: http://www.oeidrus-bc.gob.mx/oeidrus_bca/pdf/biblioteca/panoramas/2015/FICHA%20SAN%20QUINTIN%202015.pdf. Accessed: 02/20/2018.
Shen, C., Zhang, C., Xin, P., Kong, J., Li, L., 2018. Salt dynamics in coastal marshes: formation of hypersaline zones. Water Resour. Res. 54, 1–18. https://doi.org/10.1029/2017WR022021.
SMN, 2018. Normales climatológicas por estación. Sistema Meteorológico Nacional, Santa María del Mar 2063, Baja California, México. Available from: http://smn.cna.gob.mx/. Accessed: 09/02/2018.
Spalding, M., Taylor, M., Ravilious, C., Green, E., Short, F., 2003. Global overview the distribution and status of seagrasses. In Green, E. P., Short, F. T., (eds) World Atlas of Seagrasses. UNEP World Conservation Monitoring Centre. University of California Press, Berkeley. USA. 5–26.
Thorhaug, A.L., Poulos, H.M., López-Portillo, J., Barr, J., Lara-Domínguez, A.L., Ku, T.C., Graeme, P.B., 2019. Gulf of Mexico estuarine blue carbon stock, extent and flux: mangroves, marshes, and seagrasses: a North American hotspot. Sci. Tot. Environ. 653, 1253–1261. https://doi.org/10.1016/j.scitotenv.2018.10.011.
Trevathan-Tackett, S.M., Kelleway, J., Macreadie, P., Beardall, J., Ralph, P., Bellgrove, A., 2015. Comparison of marine macrophytes for their contributions to blue carbon sequestration. Ecology 96 (11), 3043–3057. https://doi.org/10.1890/15-0149.1.
Trevathan-Tackett, S.M., Macreadie, P.I., Sanderman, J., Baldock, J., Hows, J.M., Ralph, P.J., 2017a. A global assessment of the chemical recalcitrance of seagrass tissues: implications for long-term carbon sequestration. Front. Plant Sci. 8, 925. https://doi.org/10.3389/fpls.2017.00925.
Trevathan-Tackett, S.M., Wessel, C., Cebrián, J., Ralph, P.J., Masqué, P., Macreadie, P.I., 2017b. Effects of small-scale, shading-induced seagrass loss on blue carbon storage: implications for management of degraded seagrass ecosystems. J. Appl. Ecol. 55, 1351–1359. https://doi.org/10.1111/1365-2664.13081.
Turekian, K.K., Nozaki, Y., Benninger, L.K., 1977. Geochemistry of atmospheric radon and radon products. Annu. Rev. Earth Planet. Sci. 5, 227–255. https://doi.org/10.1146/annurev.ea.05.050177.00130.
Turner, R.E., Swenson, E.M., Milan, C.S., Lee, J.M., Oswald, T.A., 2004. Below-ground biomass in healthy and impaired marshes. Ecol. Res. 19, 29–35. https://doi.org/10.1111/j.1440-1703.2003.00610.x.
Ward, D.H., Morton, A., Tibbitts, T.L., Douglas, D.C., Carrera-González, E., 2003. Long-term change in eelgrass distribution at Bahia San Quintín, Baja California, Mexico, using satellite image. Estuaries 26 (6), 1529–1539. https://doi.org/10.1007/BF02803661.
Ward, D.H., Tibbitts, T.L., Morton, A., Carrera-González, E., Kempka, R., 2004. Use of digital multispectral videography to assess seagrass distribution in San Quintín Bay, Baja California, Mexico. Cienc Mar. 30 (1A), 47–60. https://doi.org/10.7773/cm.v30i11.121.
Weis, J. S., Segarra, K. E. A., Bernal, P. 2016. Salt marshes. In Inniss, L., Simcock, A., (coordinators.). The First Global Integrated Marine Assessment: World Ocean Assessment 1. United Nations, New York. Available at: http://www.un.org/Depts/los/global_reporting/WOA_RegProcess.htm. Accessed on 10/28/2018.
Zaytsev, O., Cervantes-Duarte, R., Montante, O., Gallegos-Garcia, A., 2003. Coastal upwelling activity on the Pacific shelf of the Baja California peninsula. J. Oceanogr. 59, 489–502. https://doi.org/10.1023/A:1025544700632.
Zertuche-González, J., Camacho-Ibar, V., Pacheco-Ruíz, I., Cabello-Pasini, A., Galindo-Bect, L., Guzmán-Calderón, J., Macias-Carranza, V., Espinoza-Avalos, J., 2009. The role of Ulva spp. as a temporary nutrient sink in a coastal lagoon with oyster cultivation and upwelling influence. J. Appl. Phycol. 22, 549–558. https://doi.org/10.1007/s10811-009-9491-0.